

# A Decisive Study on Dielectric Response of $\text{Bi}_2\text{O}_3$ /Polystyrene & $\text{Bi}_2\text{O}_3$ /PVDF Composite as Flexible Electrodes for Energy Storage

Dinesh Kumar Yadav<sup>1</sup>, Anju Yadav<sup>1</sup>, Sushil Kumar Jain<sup>2</sup>, Narendra Jakhar<sup>1</sup>, Balram Tripathi<sup>3,4</sup>

<sup>1</sup>Department of Physics, University of Rajasthan Jaipur, Rajasthan, India

<sup>2</sup>Department of Physics, School of Basic Science, Manipal University Jaipur, Jaipur, India

<sup>3</sup>Department of Physics, S S Jain Subodh PG (Auto.) College Jaipur, Rajasthan, India

<sup>4</sup>Department of Physics, University of Puerto Rico, Sam Juan, PR, USA

Email: balram.tripathi@upr.edu

**How to cite this paper:** Yadav, D.K., Yadav, A., Jain, S.K., Jakhar, N. and Tripathi, B. (2023) A Decisive Study on Dielectric Response of  $\text{Bi}_2\text{O}_3$ /Polystyrene &  $\text{Bi}_2\text{O}_3$ /PVDF Composite as Flexible Electrodes for Energy Storage. *Open Journal of Composite Materials*, 13, 1-11.

<https://doi.org/10.4236/ojcm.2023.131001>

**Received:** October 12, 2022

**Accepted:** December 31, 2022

**Published:** January 3, 2023

Copyright © 2023 by author(s) and Scientific Research Publishing Inc.

This work is licensed under the Creative

Commons Attribution International

License (CC BY 4.0).

<http://creativecommons.org/licenses/by/4.0/>



Open Access

## Abstract

In this manuscript a comparative study on  $\text{Bi}_2\text{O}_3$ /polystyrene and  $\text{Bi}_2\text{O}_3$ /PVDF composites has been executed via analysis of structural, bonding, surface morphology and dielectric response of composites for energy storage. The composites have been synthesized using solution cast method by varying concentrations of  $\text{Bi}_2\text{O}_3$  (BO = 1 - 5 mw%) into polystyrene (PS) and polyvinylidene fluoride (PVDF) polymers respectively. X-ray diffraction confirms the generation of crystallinity, Fourier transform infrared (FT-IR) spectroscopy confirms bonding behavior and scanning electron microscopy (SEM) confirms uniform distribution of  $\text{Bi}_2\text{O}_3$  (BO) in PS and PVDF polymers. Impedance spectroscopy has been employed for determination of dielectric response of the fabricated composites. The dielectric constant has been found to be increased as 1.4 times of pristine PS to  $\text{BO}_{5\%}\text{PS}_{95\%}$  composites and 1.8 times of pristine PVDF to  $\text{BO}_{5\%}\text{PVDF}_{95\%}$  composites respectively. These high dielectric composite electrodes are useful for flexible energy storage devices.

## Keywords

Bismuth Oxide ( $\text{Bi}_2\text{O}_3$ ), Polymer Composites, Surface Morphology, Dielectric Constant, Energy Storage

## 1. Introduction

Flexible supercapacitors are highly attractive for the large number of emerging portable lightweight consumer devices. The novelty of a flexible super capacitor is the incorporation of flexible electrode or substrate material to combine struc-

tural flexibility with the inherently high power density of supercapacitors. Flexible supercapacitors can use non-Faradaic energy storage process as seen in the electric double layer capacitor type or a Faradaic mechanism as seen in the pseudocapacitors (PCs). Materials with high dielectric constant attracted attention of researchers due to their suitability for energy storage applications. [1] [2] Generally, dielectric constant of pristine polymers is low, however these materials have drawn considerable interest for energy storage applications due to their easy processing, low cost, high breakdown strength and light weight. [3] [4] [5] If the permittivity of these polymeric materials could be increased then they might be suitable materials for energy storage applications. The loading of ceramic fillers increases permittivity of polymers. [6] [7] To attain this kind of materials, high dielectric constant ceramic fillers like bismuth oxide ( $\text{Bi}_2\text{O}_3$ ) loaded into polymers like polystyrene (PS) and polyvinylidene fluoride (PVDF) because of their extraordinary thermal, chemical, dielectric, pyroelectric, mechanical and piezoelectric properties. PS is naturally transparent, thermoplastic, waterproof, dimensionally stable, rigid chemical inert, relatively cheaper, versatile, good dielectric strength and easy to fabricate. [8] PVDF has incredible properties such as excellent mechanical strength, light weight, heat, radiation and weather resistant, recyclable and easy to process. The polarity of alternating  $\text{CH}_2$  and  $\text{CF}_2$  groups present in PVDF  $(\text{C}_2\text{H}_2\text{F}_2)_n$  chains are responsible for its amazing electrical properties. [9] [10] The dielectric constant of pristine PS and PVDF is 2.5 and 10 respectively at room temperature and at KHz frequencies. [11] [12] [13] Dielectric strength of PS and PVDF is 19.7 MV/m and 420 MV/m respectively. [14] [15]  $\text{Bi}_2\text{O}_3$  is a metal oxide suitable as filler due to its high dielectric constant as well as good photoelectric, mechanical and electrical properties. The  $\alpha$ - $\text{Bi}_2\text{O}_3$  phase is most stable and commonly used in ceramic applications [16]. Permittivity of the ceramic/polymer composites increases with filler concentration, however decreases in breakdown strength and mechanical properties which limits high concentration of filler. [17] [18] [19] [20] In present work, a comparative study on structure, surface morphology, bonding and dielectric response has been executed for BO/PS and BO/PVDF composites with varying filler concentration to optimize the best concentration of loading where high dielectric constant is achieved without losing the other responses.

## 2. Experimental

### 2.1. Materials

Bismuth oxide ( $\text{Bi}_2\text{O}_3$  99.99% purity), polystyrene (PS) granules purchased from Sigma Aldrich, polyvinylidene fluoride (PVDF 99.99%) & solvents like dichloromethane, NMP and benzene were purchased from Alfa Aesar respectively.

### 2.2. Synthesis of Composites

The BO/PS and BO/PVDF composites with varying concentration of BO = 1 to 5 wt% were synthesized by solution casting method. In this method, filler and po-

lymers were individually dispersed in crystallizable benzene using ultrasonicator for one hour. Then both the solutions were mixed and further sonicated till homogeneously dispersion. This mixed solution was poured in the Petri dish floating on mercury surface to get composites of uniform thickness of 100  $\mu\text{m}$ .

### 2.3. Characterization

X-ray diffractometer (Bruker AXS, ApexII) in the angle ( $2\theta$ ) range  $20^\circ$  to  $60^\circ$  with step resolution  $0.2^\circ$  was used to investigate the structure of the composites. FT-IR spectra of all synthesized composites were collected by using Alpha Bruker FT-IR Spectrometer (ECO-ATR) in wave number range  $4000\text{ cm}^{-1}$  to  $500\text{ cm}^{-1}$  at room temperature. Scanning electron microscope JSM-7610F Plus, JEOL Ltd Tokyo, was used for surface morphology and energy dispersive x-ray (EDX) spectra for elemental analysis of the fabricated composites. Impedance analyzer WAYNE KERR Electronics, London, UK (6500B series) was used for dielectric response measurements in the frequency range 1 kHz to 3.16 MHz.

## 3. Results and Discussion

### 3.1. X-Ray Diffraction

**Figure 1** show XRD spectra of pristine PS, PVDF, BO,  $\text{BO}_{1\%}\text{PS}_{99\%}$ ,  $\text{BO}_{5\%}\text{PS}_{95\%}$ ,  $\text{BO}_{1\%}\text{PVDF}_{99\%}$  and  $\text{BO}_{5\%}\text{PS}_{95\%}$  composites. The average crystallite size of the order of 50 nm for  $\text{Bi}_2\text{O}_3$  has been found by Scherer equation.

The diffraction spectrum of bismuth oxide shows peaks at angles  $27.3^\circ$ ,  $33.1^\circ$ ,  $46.4^\circ$  and  $54.8^\circ$  corresponds to planes (120), (121), (311) and (241) respectively

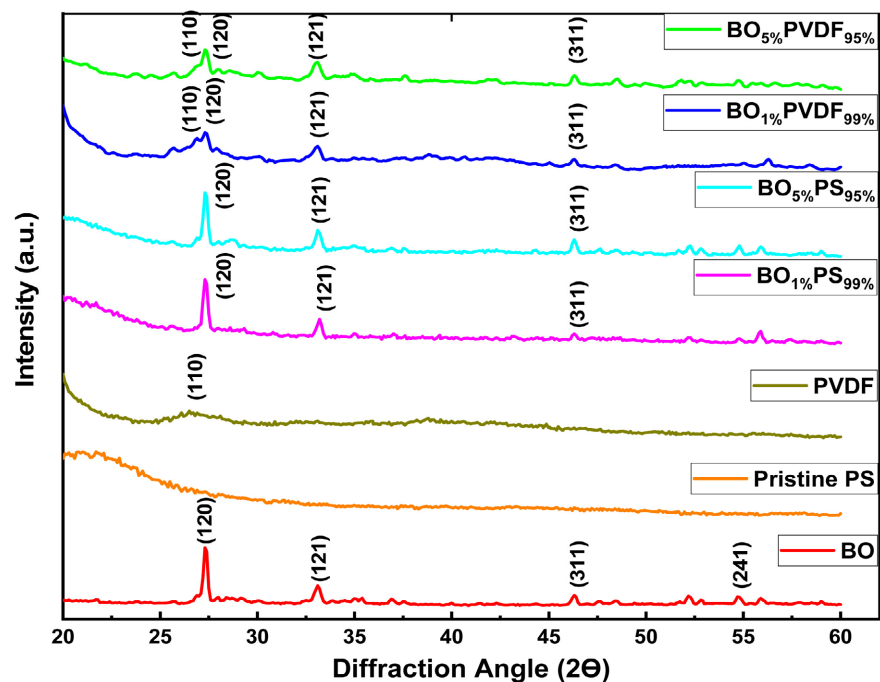


**Figure 1.** XRD spectra for (a) BO, (b) pristine PS, (c) PVDF, (d)  $\text{BO}_{1\%}\text{PS}_{99\%}$ , (e)  $\text{BO}_{5\%}\text{PS}_{95\%}$ , (f)  $\text{BO}_{1\%}\text{PVDF}_{99\%}$  and (g)  $\text{BO}_{5\%}\text{PVDF}_{95\%}$ . Composites.

matches well with JCPDS file (76 - 1730) belongs to monoclinic phase of  $\text{Bi}_2\text{O}_3$  [21] [22]. XRD spectrum of pristine PS showed only a hump reflecting amorphous nature of polystyrene. [23] However diffraction peaks at  $2\theta = 26.4^\circ$ ,  $34^\circ$  and  $46^\circ$  are obtained for PVDF, [24] showing the crystalline nature of the polymer. The position of diffraction peaks for composites like  $\text{BO}_{1\%}\text{PS}_{99\%}$ ,  $\text{BO}_{5\%}\text{PS}_{95\%}$ ,  $\text{BO}_{1\%}\text{PVDF}_{99\%}$  and  $\text{BO}_{5\%}\text{PVDF}_{95\%}$  composites remains the same as those of individual only intensities at higher concentration of filler found to be increased indicating the phases of dispersed bismuth oxide.

### 3.2. SEM and EDX Analysis

Figures 2(a)-(i) show SEM images of pristine PS, PVDF,  $\text{Bi}_2\text{O}_3$ , BO/PS and BO/PVDF composites at different magnifications. The surface morphology of pristine PS as shown in Figure 2(a) looks like colloidal structure, however SEM images of PVDF Figure 2(b) and Figure 2(c) appearing like spherical ball shape connected to each other. The SEM micrographs as shown in Figure 2(d) and Figure 2(e) appearing like cylindrical needle shape of bismuth oxide ( $\text{Bi}_2\text{O}_3$ ) match well with previous reports. [25] [26] The porous structure formation in BO/PS composites as shown in Figure 2(f) and Figure 2(g), may help to trap

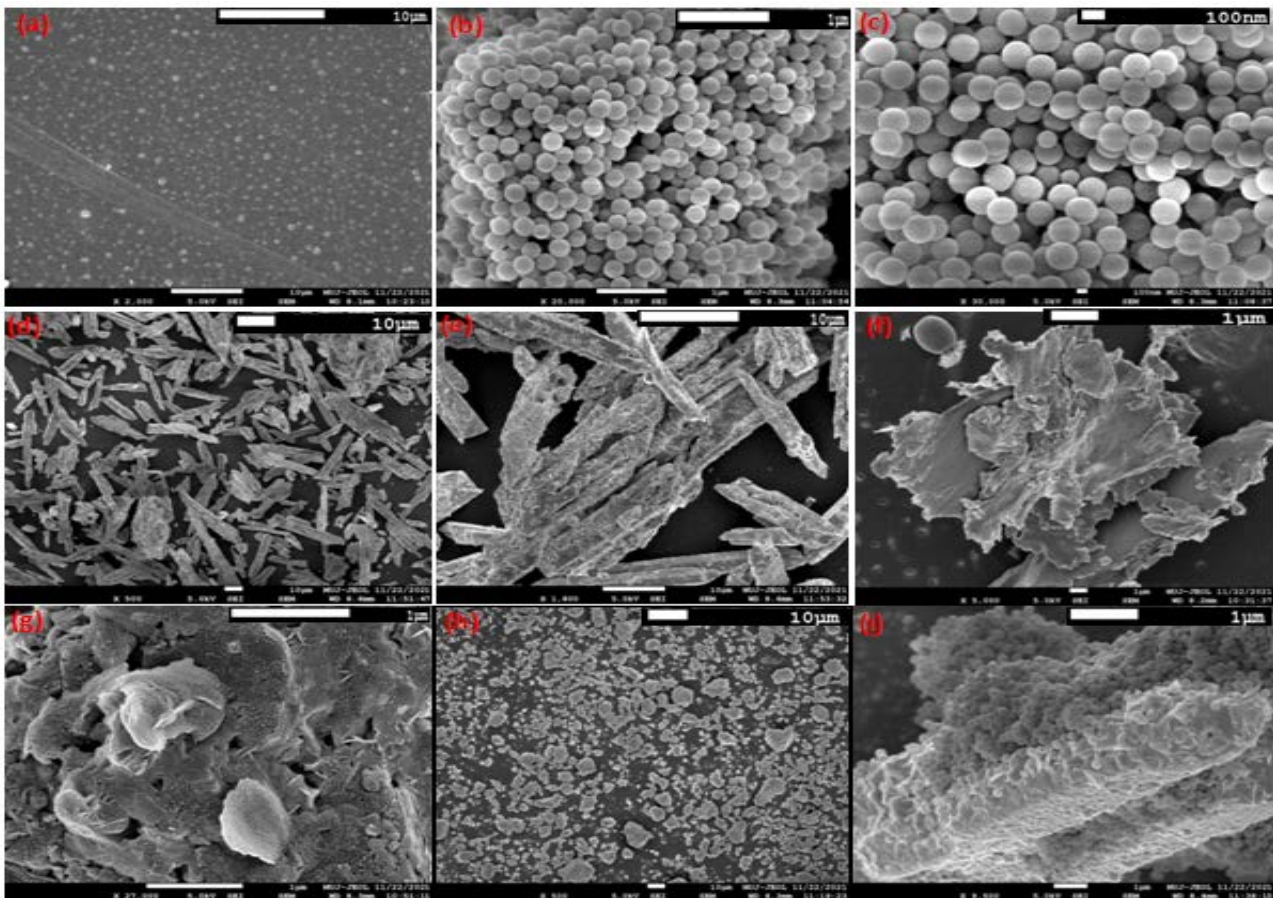


**Figure 2.** SEM images for (a) pristine PS ((b) & (c)) PVDF ((d) and (e)),  $\text{Bi}_2\text{O}_3$  ((f) and (g)), BO/PS ((h) and (i)) BO/PVDF composites.

charge carriers during charge discharge process. The rods of BO surrounded by PVDF as shown in **Figure 2(h)** and **Figure 2(i)** represents a significant interaction between filler and polymer which has been also obtained by bonding characteristics as confirmed by FT-IR measurements.

**Figure 3(a)** and **Figure 3(b)** represents energy dispersive x-ray spectra of BO/PS & BO/PVDF composites, confirms presence of bismuth, oxygen, and carbon in the fabricated composites of PS and PVDF. [27]

### 3.3. FT-IR Spectroscopy

**Figure 4(a)** and **Figure 4(b)** show FT-IR spectra for pristine BO, PS, BO/PVDF composites and BO, PS, BO/PS composites. As shown in **Figure 4**, peaks for BO are observed at  $563\text{ cm}^{-1}$ ,  $604\text{ cm}^{-1}$ ,  $1535\text{ cm}^{-1}$ ,  $1685\text{ cm}^{-1}$  and around  $3600\text{ cm}^{-1}$  corresponds to Bi-O stretch, Bi-O-Bi (metal-oxygen-metal) stretching vibrations,  $\text{NO}_3^-$  group and O-H (hydroxyl group) stretching respectively. These peaks are reference of monoclinic structure of  $\text{Bi}_2\text{O}_3$ , and matches well with earlier reports [28]. As shown in **Figure 4(a)**, absorption peaks at  $604\text{ cm}^{-1}$ ,  $760\text{ cm}^{-1}$  ( $\text{CF}_2$  bending),  $871\text{ cm}^{-1}$  (C-C-C),  $1173\text{ cm}^{-1}$  ( $\text{CF}_2$  stretch),  $1395\text{ cm}^{-1}$  ( $\text{CH}_2$  wagging) and  $1685\text{ cm}^{-1}$  (C = C stretching vibration) are characteristic peaks of  $\alpha$ -PVDF. Appearance of absorption peaks at the same wave number in composites and individual is evidence of well orientation and bonding of filler with PVDF. FT-IR spectrum of pristine PS as shown in **Figure 4(b)** showing various peaks at wavenumbers like  $684\text{ cm}^{-1}$ ,  $754\text{ cm}^{-1}$ ,  $1494\text{ cm}^{-1}$ , and  $3026\text{ cm}^{-1}$  related to C-H bending, aromatic C = C stretching and aromatic C-H stretching vibrations and characteristic peak of styrene [29].

### 3.4. Dielectric Spectroscopy

**Figure 5(a)** and **Figure 5(b)** show frequency vs dielectric constant of pristine PVDF as well as BO/PVDF composites and PS as well as BO/PS composites. The dielectric constant of pristine PS is obtained 3.687 at freq. of 1 kHz and found to be increased for  $\text{BO}_{5\%}\text{PS}_{95\%}$ . up to 5.246, similarly, dielectric constant of PVDF is obtained 9.754 and found to be increased for  $\text{BO}_{5\%}\text{PVDF}_{95\%}$  upto 17.449 attributes

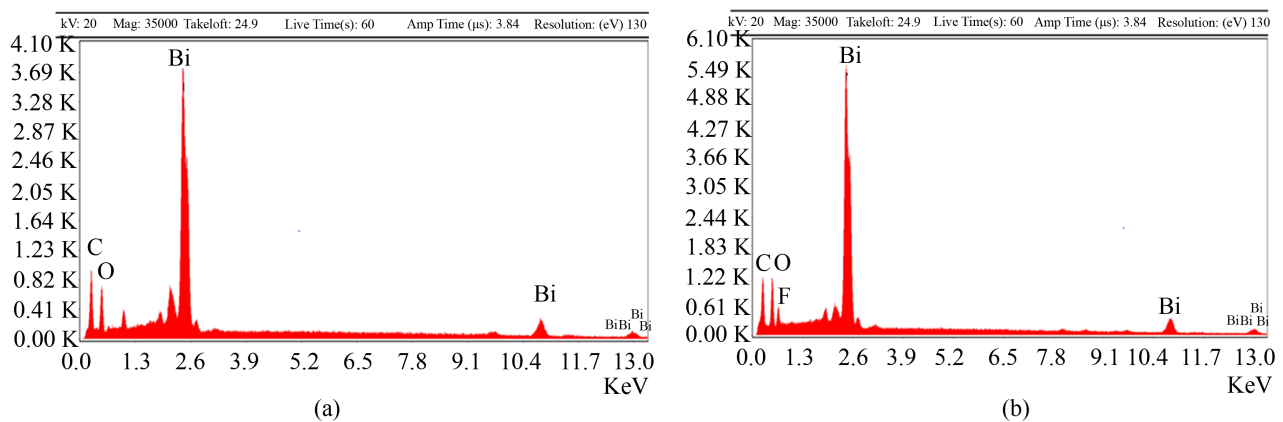


**Figure 3.** EDX spectra for (a) BO-PS and (b) BO-PVDF composites.



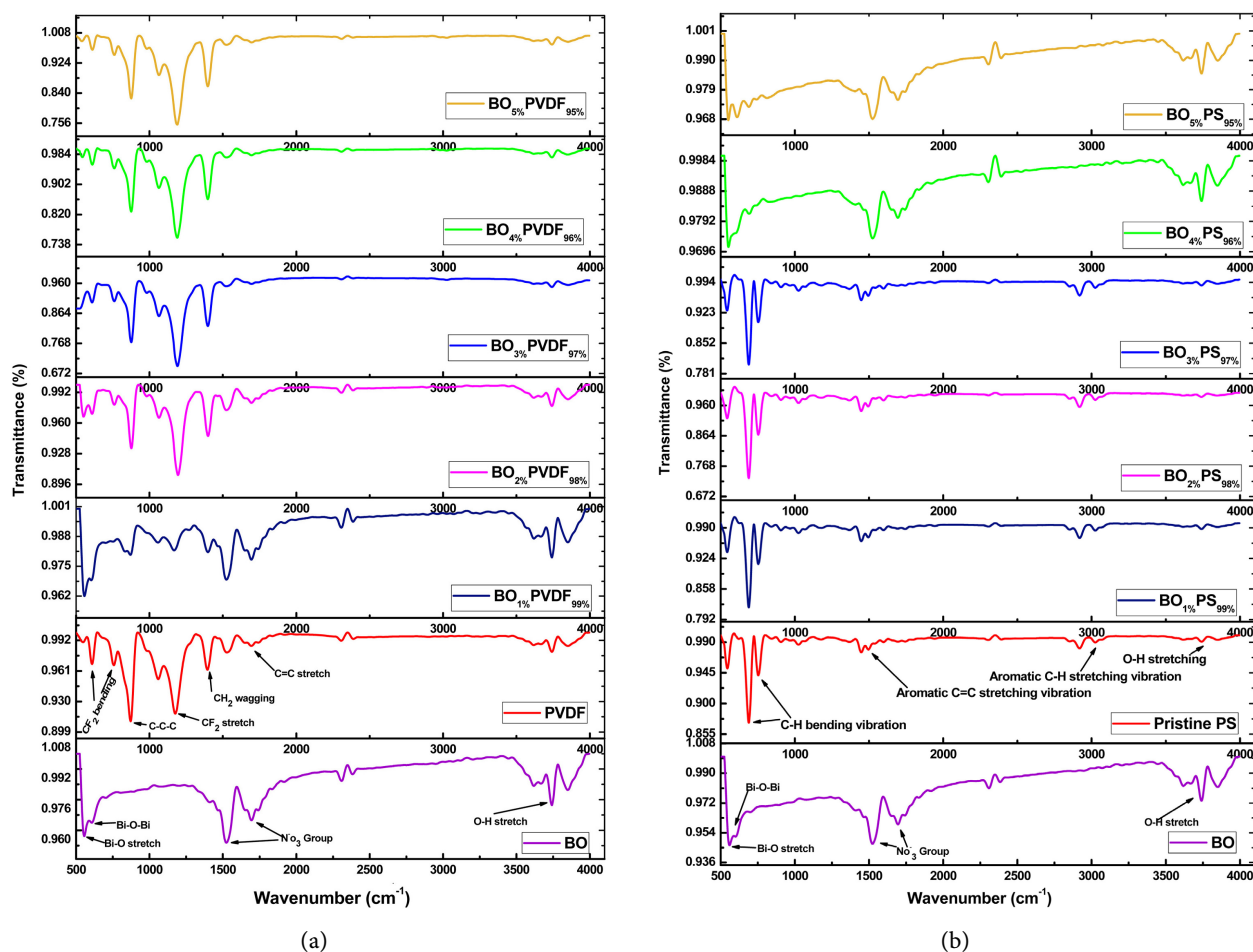


**Figure 4.** FT-IR spectra for (a) BO, PVDF & BO/PVDF composites; (b) BO, pristine PS & BO/PS composites.

the accumulation of charge at grain boundaries leading to the formation of intrinsic dipoles in composites of BO/PS and BO/PVDF results dielectric constant approx. equivalent to the BO. Thus, on increasing BO concentration within the polymers, there might be maximum possibility of increase in intrinsic dipoles and polarization area of the composites, which results as enhancement in dielectric constant. However, values of dielectric constant decreases with increase of frequency attributes all type of polarization (interfacial, dipolar, vibrational and electronic polarization) contributes in permittivity, but dipoles are unable to flip with field when frequency is increased causing the polarization and dielectric constant to decrease with increasing frequency. [30]

**Figure 6(a)** and **Figure 6(b)** show dissipation factor ( $\tan\delta$ ) vs frequency response of pristine PVDF, BO/PVDF composites as well as PS, and BO/PS composites respectively. It indicates that  $\tan\delta$  increases with increasing BO concentration in both the polymers PS and PVDF. Dissipation factor attains large values for BO<sub>5%</sub>PS<sub>95%</sub> and BO<sub>5%</sub>PVDF<sub>95%</sub> composites. As shown in **Figure 6(b)**, PS and BO/PS composites have large  $\tan\delta$  values at smaller frequencies and decreases with frequency up to 500 kHz, after this it increases again with increasing frequency.

However, for PVDF and BO/PVDF composites  $\tan\delta$  decreases with frequency up to 100 kHz and then increases rapidly with increasing frequency, as shown in **Figure 6(a)**. The dielectric constant of BO<sub>5%</sub>PS<sub>95%</sub> and BO<sub>5%</sub>PVDF<sub>95%</sub> composites increased 1.4 and 1.8 times as compared to pristine PS and PVDF which is very close to the reports available in the literature [31]. Thus, filler BO improves dielectric performance of composites but dissipation factor limits its concentration. **Table 1** showed values of dielectric constant with log f for pristine PS & PVDF as well as their various composites.

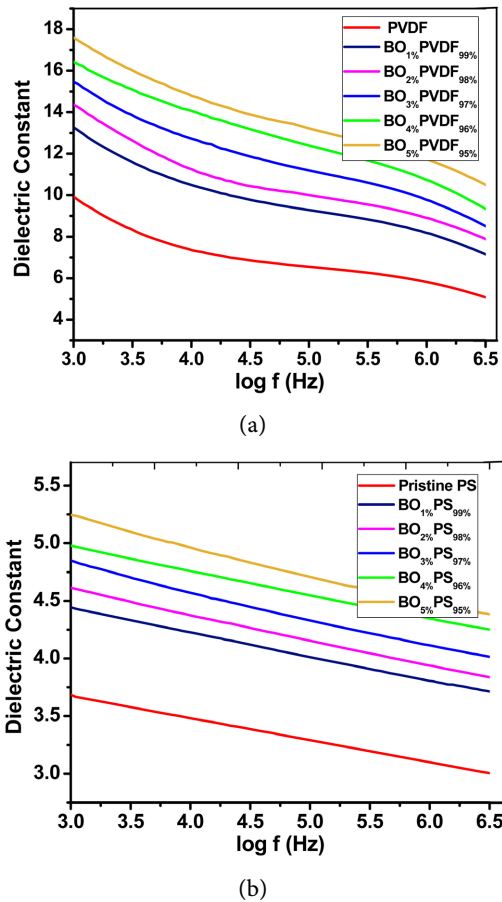


**Figure 5.** Dielectric constant vs frequency response of (a) pristine PVDF & BO/PVDF composites; (b) pristine PS & BO/PS composites.

**Table 1.** Values of dielectric constant with log f for pristine PS & PVDF as well as their various composites.

S. No.	log f (Hz)	Dielectric Constant							
		Pristine PS	BO <sub>1%</sub> PS <sub>99%</sub>	BO <sub>3%</sub> PS <sub>97%</sub>	BO <sub>5%</sub> PS <sub>95%</sub>	PVDF	BO <sub>1%</sub> PVDF <sub>99%</sub>	BO <sub>3%</sub> PVDF <sub>97%</sub>	BO <sub>5%</sub> PVDF <sub>95%</sub>
1	3.0000	3.687	4.445	4.851	5.246	9.754	13.118	15.347	17.449
2	4.0101	3.478	4.225	4.567	4.961	7.348	10.469	12.703	14.772
3	5.0202	3.288	4.007	4.326	4.703	6.539	9.265	11.168	13.188
4	6.0303	3.094	3.801	4.108	4.476	5.785	8.140	9.715	11.663
5	6.5000	3.001	3.710	4.012	4.380	5.062	7.120	8.476	10.456

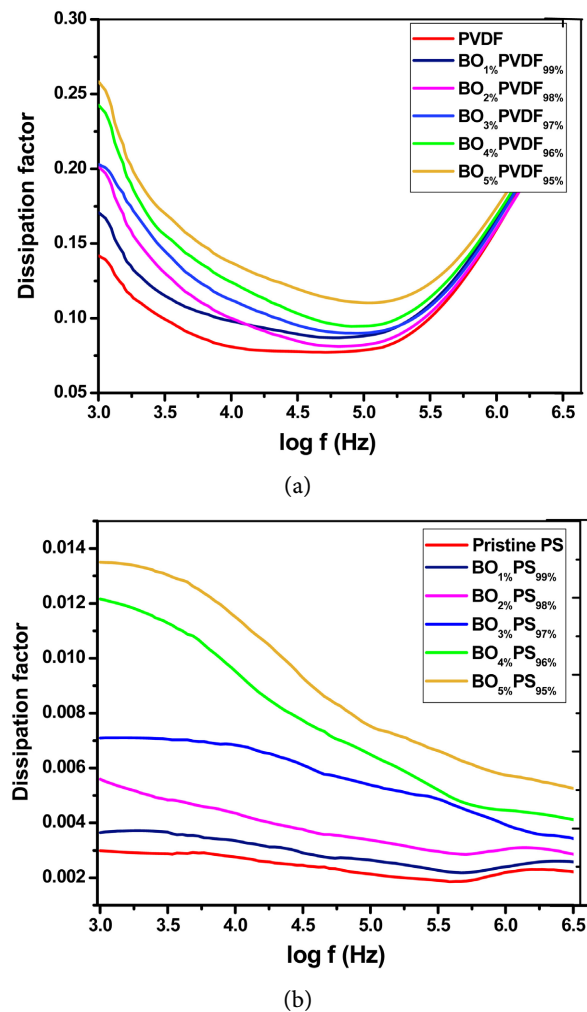


**Figure 6.** Dissipation factor vs frequency response of (a) pristine PVDF & BO/PVDF composites (b) PS & BO/PS composites.

#### 4. Conclusion

In summary, the average crystallite size of bismuth oxide has been found approx. 50 nm which was used as filler in the PS and PVDF matrix. The XRD spectra of bismuth oxide and PVDF are consistent to monoclinic crystal structure, however spectrum for PS indicated its amorphous nature. SEM micrographs showed well orientation of BO in PS and PVDF composites however FT-IR spectra reveal good interaction between filler and polymers in composites. The dielectric constant of  $\text{BO}_{5\%}\text{PS}_{95\%}$  and  $\text{BO}_{5\%}\text{PVDF}_{95\%}$  composites increased 1.4 and 1.8 times to that of pristine PS and PVDF respectively and attributes the accumulation of charge at grain boundaries leading to the formation of intrinsic dipoles in composites of BO/PS and BO/PVDF. These types of enhanced dielectric constant composites are useful in flexible energy storage devices.

#### Acknowledgements

Authors are thankful to DST, SERB-DST & DBT New Delhi for support under



SR/FST/College/2020/1003, TAR/2022/000432, & DBT star (BT/HRD/023/11/2019), Central Analytical Facilities Manipal University, Jaipur for providing SEM, FT-IR facility and IIT Jodhpur for providing XRD facility.

## Conflicts of Interest

The authors declare no conflicts of interest regarding the publication of this paper.

## References

- [1] Wang, D., Huang, M.Y., Zha, J.-W., Zhao, J., Dang, Z.-M. and Cheng, Z.Y. (2014) Dielectric Properties of Polystyrene Based Composites Filled with Core-Shell Ba-TiO<sub>3</sub>/Polystyrene Hybrid Nanoparticles. *IEEE Transactions on Dielectrics and Electrical Insulation*, **21**, 1438-1445. <https://doi.org/10.1109/TDEI.2013.004329>
- [2] Barber, P., Balasubramanian, S., Anguchamy, Y., Gong, S., Wibowo, A., Gao, H., Ploehn, H. and Loye, H. (2009) Polymer Composite and Nanocomposite Dielectric Materials for Pulse Power Energy Storage. *Materials*, **2**, 1697-1733. <https://doi.org/10.3390/ma2041697>
- [3] Mao, X., Guo, W.F., Li, C.Z., Yang, J., Du, L., et al. (2017) Low-Temperature Synthesis of Polyimide/Poly (Vinylidene Fluoride) Composites with Excellent Dielectric Property. *Materials Letters*, **5**, 193-213. <https://doi.org/10.1016/j.matlet.2017.01.065>
- [4] Ramadan, K.S., Sameoto, D. and Evoy, S. (2014) A Review of Piezoelectric Polymers as Functional Materials for Electromechanical Transducers. *Smart Materials and Structures*, **23**, Article ID: 033001. <https://doi.org/10.1088/0964-1726/23/3/033001>
- [5] Samanta, B., Kumar, P., Nanda, D. and Sahu, R. (2019) Dielectric Properties of Epoxy-Al Composites for Embedded Capacitor Applications. *Result in Physics*, **14**, Article ID: 102384. <https://doi.org/10.1016/j.rinp.2019.102384>
- [6] Rao, Y., Ogitali, S., Kohl, P. and Wong, C.P. (2002) Novel Polymer-Ceramic Nanocomposite Based on High Dielectric Constant Epoxy Formula for Embedded Capacitor Application. *Journal of Applied Polymer Science*, **83**, 1084-1090. <https://doi.org/10.1002/app.10082>
- [7] Subodh, G., Deepu, V., Mohanan, P. and Sebastian, M. (2009) Dielectric Response of High Permittivity Polymer Ceramic Composite with Low Loss Tangent. *Applied Physics Letters*, **95**, Article ID: 062903. <https://doi.org/10.1063/1.3200244>
- [8] Xiao, M., Sun, L., Liu, J., Li, Y. and Gong, K. (2002) Synthesis and Properties of Polystyrene/Graphite Nanocomposites. *Polymer*, **43**, 2245-2248. [https://doi.org/10.1016/S0032-3861\(02\)00022-8](https://doi.org/10.1016/S0032-3861(02)00022-8)
- [9] Li, N., Xiao, C.F., An, S.L. and Hu, X.Y. (2010) Preparation and Properties of PVDF/PVA Hollow Fiber Membranes. *Desalination*, **250**, 530-537. <https://doi.org/10.1016/j.desal.2008.10.027>
- [10] Zhang, T., Huang, W., Zhang, N., Huang, T., Yang, J. and Wang, Y. (2017) Grafting of Polystyrene onto Reduced Graphene Oxide by Emulsion Polymerization for Dielectric Polymer Composites: High Dielectric Constant and Low Dielectric Loss Tuned by Varied Grafting Amount of Polystyrene. *European Polymer Journal*, **94**, 196-207. <https://doi.org/10.1016/j.eurpolymj.2017.07.008>
- [11] Yang, M., Zhao, H., Hu, C., Haghi-Ashtiani, P., He, D., Dang, Z.M. and Bai, J. (2018) Largely Enhanced Dielectric Constant of PVDF Nanocomposites through a Core-Shell Strategy. *Physical Chemistry Chemical Physics*, **20**, 2777-2786. <https://doi.org/10.1039/C7CP06510H>

- [12] Chen, H.J., Han, S., Liu, C., *et al.* (2016) Investigation of PVDF-TrFE Composite with Nanofillers for Sensitivity Improvement. *Sensors and Actuators A: Physical*, **245**, 135-139. <https://doi.org/10.1016/j.sna.2016.04.056>
- [13] Aatur Rahman, M. and Chung, G.S. (2013) Synthesis of PVDF-Graphene Nanocomposites and Their Properties. *Journal of Alloys and Compounds*, **581**, 724-730. <https://doi.org/10.1016/j.jallcom.2013.07.118>
- [14] Yang, Z., Wang, J., Hu, Y., Deng, C., Zhu, K. and Qiu, J. (2020) Simultaneously Improved Dielectric Constant and Breakdown Strength of PVDF/Nd-BaTiO<sub>3</sub> Fiber Composite Films via the Surface Modification and Subtle Filler Content Modulation. *Composites Part A: Applied Science and Manufacturing*, **128**, Article ID: 105675. <https://doi.org/10.1016/j.compositesa.2019.105675>
- [15] CRC Handbook of Chemistry and Physics. 102nd Edition, CRC Press, Florida.
- [16] Tezel, F.M. and Kariper, İ.A. (2017) Synthesis, Surface Tension, Optical and Dielectric Properties of Bismuth Oxide Thin Film. *Materials Science-Poland*, **35**, 87-93. <https://doi.org/10.1515/msp-2017-0020>
- [17] Bai, Y., Cheng, Z.-Y., Bharti, V., Xu, H.S., *et al.* (2000) High-Dielectric Constant Ceramic-Powder Polymer Composites. *Applied Physics Letters*, **76**, 3804-3806. <https://doi.org/10.1063/1.126787>
- [18] Cheng, K.C., Lin, C.M., Wang, S.F., Lin S.T. and Yang, C.F. (2007) Dielectric Properties of Epoxy Resin-Barium Titanate Composites at High Frequency. *Materials Letters*, **61**, 757-760. <https://doi.org/10.1016/j.matlet.2006.05.061>
- [19] Cho, S.-C., Lee, J.-Y., Hyun, J.-G. and Paik, K.-W. (2004) Study on Epoxy/BaTiO<sub>3</sub> Composite Embedded Capacitor Films (ECFs) for Organic Substrate Applications. *Materials Science and Engineering: B*, **110**, 233-239. <https://doi.org/10.1016/j.mseb.2004.01.022>
- [20] Hu, T., Juuti, J., Jantunen, H., *et al.* (2007) Dielectric Properties of BST/Polymer Composite. *Journal of the European Ceramic Society*, **27**, 3997-4001. <https://doi.org/10.1016/j.jeurceramsoc.2007.02.082>
- [21] Sindhu, S., Jabeen, F.M. and Niveditha, C.V. (2015)  $\alpha$ -Bi<sub>2</sub>O<sub>3</sub> Photoanode in DSSC and Study of the Electrode-Electrolyte Interface. *RSC Advances*, **5**, 78299-78305. <https://doi.org/10.1039/C5RA12760B>
- [22] Patterson, A.L. (1939) The Scherrer Formula for X-Ray Particle Size Determination. *Physical Review Journals Archive*, **56**, 978-982. <https://doi.org/10.1103/PhysRev.56.978>
- [23] Huang, G., Xu, J.Q., Geng, P.Y. and Li, J.H. (2020) Carrier Flotation of Low-Rank Coal with Polystyrene. *Minerals*, **10**, Article 452. <https://doi.org/10.3390/min10050452>
- [24] Ibtisam, A., Mohammad, H.J., Muhammad, Y. and Haider, S. (2015) Facile Formation of  $\beta$  Poly (Vinylidene Fluoride) Films Using the Short Time Annealing Process. *Advances in Environmental Biology*, **9**, 20-27.
- [25] Yang, Q., Li, Y.X., Yin, Q., Wang, P. and Cheng, Y.B. (2002) Hydrothermal Synthesis of Bismuth Oxide Needles. *Materials Letters*, **55**, 46-49. [https://doi.org/10.1016/S0167-577X\(01\)00617-6](https://doi.org/10.1016/S0167-577X(01)00617-6)
- [26] Yadav, D.K., Yadav, A., Meena, K., Devat, K., Mishra, J.K., Sahu, R., Jain, S.K., Dixit, A., Srivastava, N., Patodia, T., Jakhar, N. and Tripathi, B. (2021) Study of CNT Intercalated Bi<sub>2</sub>O<sub>3</sub>/PVDF Composite for Super Capacitors Applications. *Macromolecular Symposia*, **399**, Article ID: 2100022. <https://doi.org/10.1002/masy.202100022>
- [27] Sahu, R., Patodia, T., Yadav, D., Jain, S.K. and Tripathi, B. (2022) Visible-Light In-

- duced Photo Catalytic Response of MWCNTs-CdS Composites via Efficient Interfacial Charge Transfer. *Materials Letters. X*, **13**, Article ID: 100116. <https://doi.org/10.1016/j.mlblux.2021.100116>
- [28] Vinodh, R., Abidov, A., Peng, M.M., Babu, C.M., Palanichamy, M., *et al.* (2015) A New Strategy to Synthesize Hypercross-Linked Conjugated Polystyrene and Its Application towards CO<sub>2</sub> Sorption. *Fibers and Polymers*, **16**, 1458-1467. <https://doi.org/10.1007/s12221-015-5151-y>
- [29] Xia, W.M. and Zhang, Z.C. (2018) PVDF-Based Dielectric Polymers and Their Applications in Electronic Materials. *IET Nanodielectrics*, **1**, 17-31. <https://doi.org/10.1049/iet-nde.2018.0001>
- [30] Yadav, A., Mishra, J., Sahu, R., Jain, S.K., Dixit, S., Agarwal, G., Jakhar, N. and Tripathi, B. (2021) Effect of BaTiO<sub>3</sub> Nanofillers on the Energy Storage Performance of Polymer Nanocomposites. *Macromolecular Symposia*, **399**, Article ID: 2100024. <https://doi.org/10.1002/masy.202100024>
- [31] Matysiak, V. (2022) Synthesis of 1D Bi<sub>2</sub>O<sub>3</sub> Nanostructures from Hybrid Electro Spun Fibrous Mats and Their Morphology, Structure, Optical and Electrical Properties. *Scientific Reports*, **12**, Article No. 4046. <https://doi.org/10.1038/s41598-022-07830-z>